Princeton Plasma Physics Laboratory

PPPL- 4363

PPPL- 4363

Fusion-born Alpha Particle Ripple Loss Studies in ITER

G.J. Kramer, R.B. White, R. Nazikian, H.L. Berk

March, 2009

PPPL
PRINCETON PLASMA
PHYSICS LABORATORY

Prepared for the U.S. Department of Energy under Contract DE-AC02-76CH03073.

Fusion-born alpha particle ripple loss studies in ITER

G.J. Kramer[1], R.B. White[1], R. Nazikian[1], H.L. Berk[21,2]

[11]*Plasma Physics Laboratory, Princeton University,*

P.O.Box 451, Princeton, New Jersey 08543

[22]*Institute for Fusion Studies, University of Texas at Austin, Austin, Texas, 78712*

(Dated: January 9, 2009)

Abstract

The impact of locally enhanced toroidal magnetic field ripple due to three test blanket modules (TBMs) on fusion-born alpha particles is studied for two standard ITER scenarios. Only the (peaked) alpha particle birth profiles were taken into account without redistribution due to MHD activity. It was found that the inclusion of TBMs enhance the losses by up to 35% compared to the losses found for a toroidal field ripple of 0.2% optimized with ferritic inserts. Without TBMs the losses are spread uniformly over the first wall giving alpha particle heat loads of 10 kW/m^2. When the TBMs are included localized losses ocur in front of the TBMs with heat loads of up to 60 kW/m^2 which is well below the 500 kW/m^2 design value for the ITER first wall. We therefore conclude that ripple fields induced by the TBMs do not have a significant negative impact on the fusion-born alpha particle confinement or on the heat loads of the first wall. The alpha particle fluency at the hot spots might restrict the life time of the wall because of blister formation.

PACS numbers:

I. INTRODUCTION

Fusion-born alpha particles in ITER should be confined long enough to heat the plasma and sustain the burn. A toroidal magnetic field ripple, however, can cause significant alpha particle losses before they are thermalized. Moreover, ripple-lost fusion-born alpha particles usually strike the first wall in localized regions and can create local heat loads that approach or exceed the design value for the first wall. Therefore, it is important to design the toroidal magnetic field in such a way that the field ripple is sufficiently low to confine the alpha particles well and avoid excessive heat loads on the plasma facing components.

A major goal on ITER is to study tritium breeding in blanket modules. Three test blanket modules (TBMs) are being envisioned for ITER. These TBMs contain a significant amount of ferritic steel, in some of the current designs up to 2 tons, and therefore, the TBMs will modify the toroidal field ripple significantly. The TBMs will be inserted at the mid-plane at three toroidal angles, -40, 0, and 40 deg. and they have a significant impact on the toroidal field ripple as can be seen in fig. 1 [1]. The 18-fold toroidal symmetry is broken and three strong magnetic perturbations are created in front of the TBMs that can affect the fusion-born alpha particle confinement negatively.

Fusion-born Alpha particle losses have been studied in the past in order to obtain the heat loads on plasma facing components due to ripple induced losses [2, 3]. In those studies

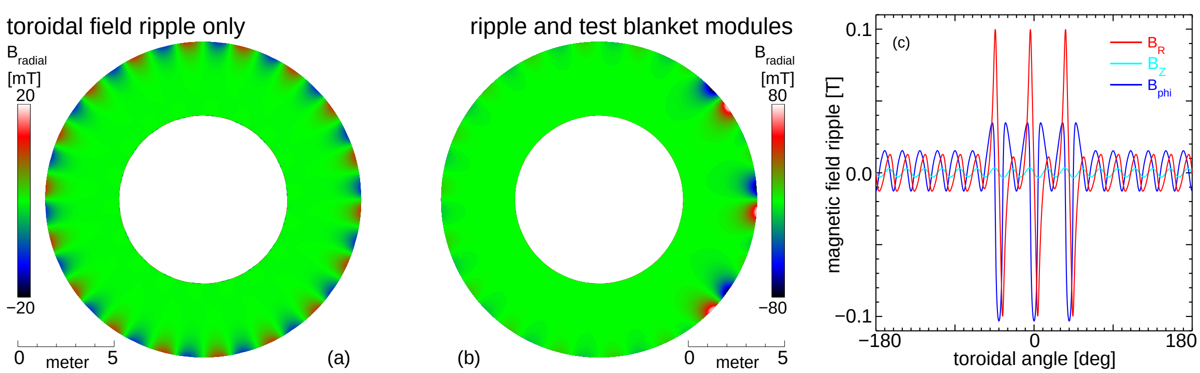

FIG. 1: *Radial component of the ITER toroidal field ripple with ferritic inserts included. In (a) the ripple without and in (b) the ripple with three TBMs is shown while in (c) the radial, vertical and toroidal magnetic field components at the LCF mid plane at R=8.28 m and Z=0.60 m are shown. Note the four fold increase of the color scale between (a) and (b).*

it was found that when the toroidal field ripple was reduced to 0.2% at the last closed flux surface (LCF), by using ferritic inserts between the inner and outer shell of the vacuum vessel, heat loads due to fusion born alpha particles can be kept well within the required limits for various plasma scenarios. In those calculations only the effect of the field ripple without and with ferritic inserts was included. No calculations were done for a ripple that includes the effects of the three TBMs.

In this paper we study the effect of the increased toroidal field ripple due to the TBMs on the fusion-born alpha particle confinement for two standard ITER configurations: Scenario 2 an inductive 15 MA plasma producing 400 MW of fusion power with Q=10 for 400 s, and Scenario 4 a 9 MA steady state weakly reversed magnetic shear plasma producing 300 MW of fusion power with Q=5 for 3000 s (section II). In both cases ripple-induced fusion-born alpha particle losses were calculated without ferritic inserts, with ferritic inserts and with ferritic inserts and three TBMs (section IV). Using a harmonic decomposition of the ripple field in numerical simulations is difficult because of the large number of toroidal harmonics that has to be taken into account due to the three toroidally localized magnetic perturbations caused by the TBMs. We have therefore developed a full Lorentz particle orbit following code that can deal with non-axisymmetric ripple fields as generated by the TBMs (section III). From our simulations we have concluded that the ripple fields induced by the TBMs do not have a significant negative impact on the confinement of fusion-born alpha particles (section V) or on the first wall heat loads. The calculated alpha particle loads on the first wall, however, can cause blistering of the plasma facing components and restrict the life-time of those components significantly.

II. EQUILIBRIUM CONFIGURATIONS

We have examined the fusion-born alpha particle losses for two standard ITER configurations, Scenario 2 (fig. 2) an inductive 15 MA plasma producing 400 MW of fusion power with Q=10 for 400 s, and Scenario 4 (fig. 3) a 9 MA steady state weakly reversed magnetic shear plasma producing 300 MW of fusion power with Q=5 for 3000 s. In both cases the losses were calculated with the toroidal field ripple, and with and without the three TBMs. The two equilibrium configurations together with the alpha particle birth distributions were obtained from the ITER data base [4].

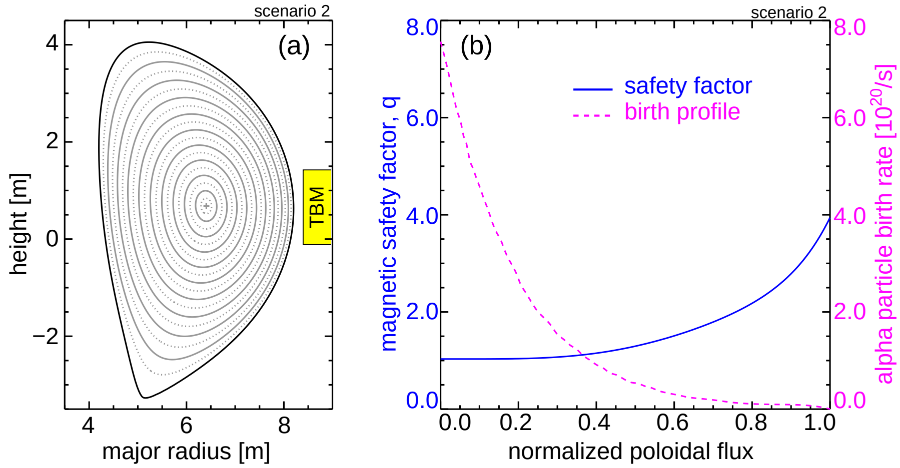

FIG. 2: *ITER equilibrium plasma configuration for scenario 2 with equispaced minor radius contours and the location of the TBMs indicated (a) and the magnetic safety factor profiles and Alpha-particle birth distributions (b).*

The 3-D magnetic ripple fields were obtained from G. Sabiene [1]. In fig. 1 the radial component of the ripple field is shown without and with the TBM ripple field included where ferritic inserts were included to reduce the toroidal field ripple at the plasma edge to 0.2% from well over 1% without ferritic inserts. The TBMs that were used in the magnetic field calculations consisted of two equal modules of 2.1 ton ferritic steel (EUFER), stacked vertically, and placed in one equatorial port. Three ports, at -40, 0, and 40 deg. toroidal angle were loaded with TBMs as is envisioned in ITER. The three components of the magnetic field ripple due to the TBMs are shown in fig. 1c at the low field-side plasma mid plane. The perturbed field due to the TBMs was calculated based on the vacuum field of ITER, not taking into account the effect of the plasma current. However, recent calculations [5] indicate that the the additional modulation of the magnetic field strength is small, so that the vacuum field calculation is adequate for a qualitative assessment of the losses.

III. SIMULATIONS

The fusion-born alpha particle loss calculations were performed with the ORBIT and SPIRAL codes. The ORBIT code is a guide center following code where the field ripple is given as a sum over a few toroidal harmonics and was used to study the cases without TBMs for benchmarking the SPIRAL code. The ORBIT code is well documented and a description

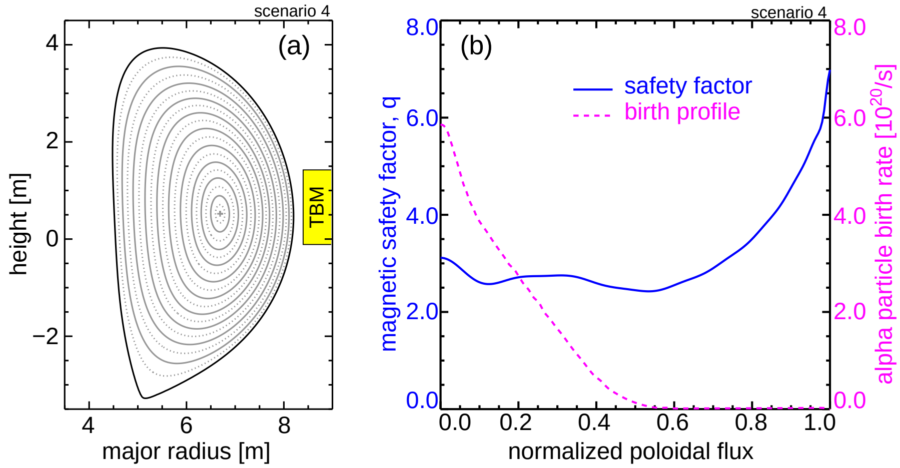

FIG. 3: *ITER equilibrium plasma configuration for scenario 4 with equispaced minor radius contours and the location of the TBMs indicated (a) and the magnetic safety factor profiles and Alpha-particle birth distributions (b).*

of the code can be found in [6, 7]. In both the ORBIT and SPIRAL code fusion-born alpha particles were drawn from the alpha-particle birth distributions (fig. 2b and 3b) and followed for a certain amount of time after their birth (up to 40 ms in the ORBIT code and 2 ms in the SPIRAL code). When a particle passed the LCF it was marked as lost.

The SPIRAL code was developed recently to study ripple fields that cannot be decomposed in one or a few dominant toroidal harmonics such as the ITER ripple field with TBMs. It solves the full Lorentz equations:

$$\vec{v} = \frac{d\vec{r}}{dt}\ ; \qquad \frac{d\vec{v}}{dt} = \frac{q}{m}\,\vec{v} \times \vec{B} \tag{1}$$

to calculate the particle orbits (with $\vec{r}$ the particle position, $\vec{v}$ its velocity, q charge, m mass, and $\vec{B}$ the magnetic field at the particle's location). A toroidally symmetric equilibrium magnetic field which contains the contributions of the plasma was obtained from an EFIT [8] calculation. EFIT gives the deviation of the toroidal magnetic field as function of the major radius, R, from the ideal field: R_0B_0/R, with B_0 the toroidal magnetic field at R_0, the plasma center, while the vertical and radial fields are obtained from the poloidal flux function, $\Psi_p(R, Z)$, (Z the vertical coordinate). This flux function is given on a rectangular grid with a resolution of approximately 2 cm. For the particle orbit calculations Ψ_p has to be interpolated between the grid points in an accurate and fast way. This was achieved as follows. The poloidal flux function was decomposed into a double sum of Chebychev polynomials of the first kind, $T(x)$, [9]:

$$\Psi_p(R,Z) = \sum_i \sum_j a_{ij} T_i(R) T_j(Z) \tag{2}$$

and usually about 30 terms are kept for each sum to give a maximum deviation of less that 0.5% between the given points and the polynomial expansion. The radial (B_R) and vertical (B_Z) magnetic fields are then obtained by taking the derivatives of eq. 2 with respect to R and Z:

$$\begin{aligned} B_R &= \frac{1}{R}\frac{\partial \Psi_p(R,Z)}{\partial Z} &&= \frac{1}{R}\sum_i \sum_j a^z_{ij} T_i(R) T_j(Z) \\ B_Z &= -\frac{1}{R}\frac{\partial \Psi_p(R,Z)}{\partial R} &&= -\frac{1}{R}\sum_i \sum_j a^r_{ij} T_i(R) T_j(Z) \end{aligned} \tag{3}$$

whereby the derivatives of the Chebychev polynomials are obtained analytically. It can be shown that the equilibrium magnetic field constructed in this way is guaranteed divergence free as required by Maxwells equations.

The toroidal ripple fields [1] that we have used in our calculations were specified as $(\tilde{B}_R, \tilde{B}_\varphi, \tilde{B}_Z)$ at 432 equally spaced toroidal angles on 1436 locations in each RZ-plane. These ripple fields were calculated for the vacuum field only. For fast and accurate calculations we have expanded the $\tilde{B}_R$ and $\tilde{B}_Z$ components of the ripple field into finite Chebychev sums similar to the equilibrium field. The $\tilde{B}_\varphi$ component is again calculated from $\tilde{B}_R$ and $\tilde{B}_Z$ to ensure that the ripple field is divergence free. For the interpolation in the toroidal direction we have used a quadratic polynomial around each given toroidal plane:

$$\tilde{B}^i_x(R,\varphi,Z) = \tilde{B}^i_x(R,Z) + U^i_x(R,Z)\varphi + V^i_x(R,Z)\varphi^2 \tag{4}$$

(with x either R or Z, and i the index of the i^{th} plane) and demand that the radial and vertical fields and their derivatives match half way between two adjacent planes. After expanding the functions $\tilde{B}^i_x(R,Z)$, $U^i_x(R,Z)$, and $V^i_x(R,Z)$ in a finite sum of Chebychev polynomials (In the current calculations 10 coefficients in the radial and 15 in the vertical direction were sufficient to describe the ripple fields accurately) the expansion coefficients can be determined uniquely from the condition that the fields be periodic in φ. From the condition that the magnetic field be divergence free the toroidal component, $\tilde{B}_\varphi$, was calculated. This involved differentiating the expansions of $\tilde{B}^i_x$, U^i_x, and V^i_x with respect to R and Z, summing the various components, and integrating with respect to φ. All those operations were performed analytically using the Chebychev expansion coefficients and therefore, the ripple field is also guaranteed to be divergence free in the calculations to the numerical precision of the computation. The analytically constructed $\tilde{B_\varphi}$ field is in excellent agreement with the given numerical one [1].

The differential equation solver that is used in the SPIRAL code is a NAG implementation [10] of a variable-order, variable-step, Adams method integrator [11]. A key feature of this integrator is that the user gives the time interval over which the equations are to be integrated together with the desired accuracy at the end of the integration. The algorithm then determines the number of steps to be taken to obtain the requested accuracy, in our case up to ten million evaluations were performed per particle followed for 2 ms. For our runs we have set the accuracy in such a way that the average particle energy was conserved by better than 0.1% with similar values for the magnetic moment. In order to assess the effects of the accuracy we have performed one run in which the energy was conserved to four parts per million at the expense of a four-fold increase in CPU time and in the number of evaluations. The losses that were found in this case and the distribution at the LCF were very similar, thereby justifying the chosen setting of the accuracy parameter.

The alpha particle birth rate is strongly peaked toward the plasma center (fig. 2 and 3) while the main losses occur from particles born near the edge (fig. 4). In order to sample the edge region with high statistical accuracy in our Monte Carlo simulations, three separate runs were performed where the particles were distributed in three plasma shells from $\Psi_{\mathrm{pol}} = [0.0, 0.25]$, $[0.25, 0.50]$, and $[0.50, 1.0]$ according to the alpha particle birth profiles and spread uniformly over the flux surface and pitch angle. In each shell at least 20000 particles were used to follow the orbits for up to 2.0 ms. Afterward, the results from the three regions were combined for further analysis and the numbers of lost particles are transformed into lost power.

IV. RESULTS

A comparison between the guide center following code ORBIT and the full Lorentz force code SPIRAL shows good agreement between the results for ITER scenario 2 in which the uncompensated ripple was used as can be seen from fig. 5 and similar results were obtained for the ripple fields that were compensated with ferritic inserts. Our loss calculations results

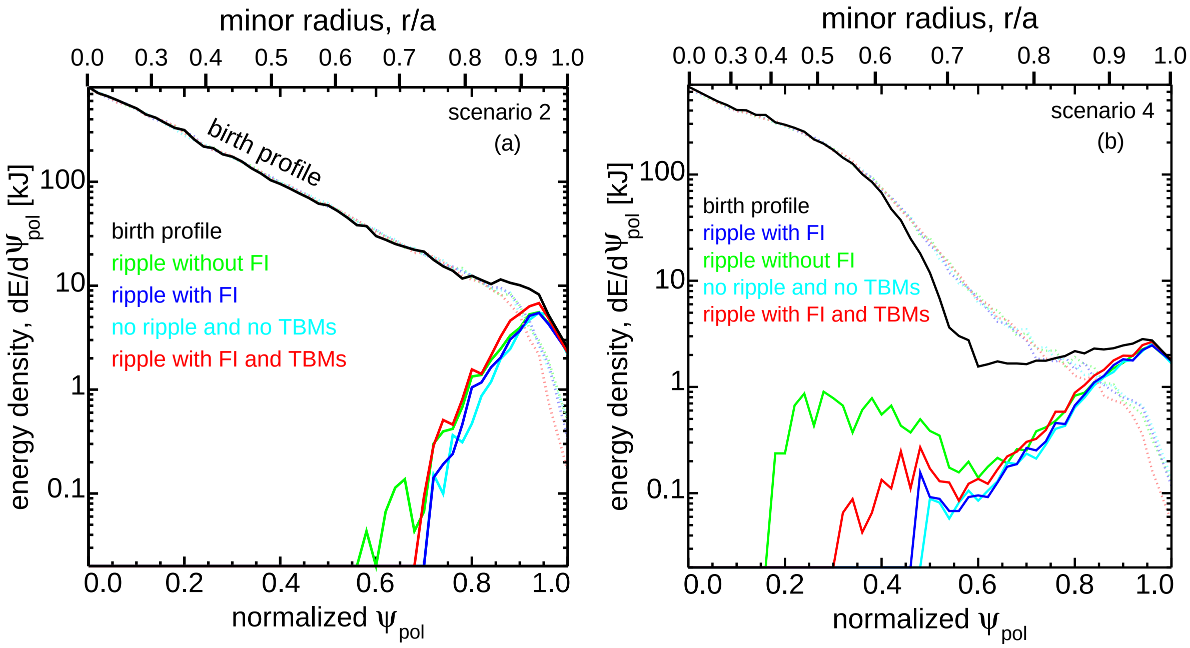

FIG. 4: *Lost alpha particle energy in 2 ms for scenario 2 (a) and scenario 4 (b) calculated with the SPIRAL code. Solid curves: losses for the the equilibrium field without ripple and without TBMs (cyan), ripple without ferritic inserts and without TBMs (green), ripple with ferritic inserts and without TBMs (blue) and ripple with ferritic inserts and TBMs. the solid black curve is the birth profile while the dotted curves are the alpha particle profiles after 2 ms (same color coding as the loss profiles).*

are similar to results from the guide center following codes ASCOT [12] and OFMC [13] and the difference might be explained by slightly different loss criteria and different assumptions on alpha particle birth profiles.

From the results of the SPIRAL code, shown in fig. 4a, it can be seen that the losses for scenario 2 come mainly from the outer layers of the plasma beyond $\Psi_{\rm pol} = 0.7$ (or $r/a = 0.72$). The losses calculated without any field ripple (cyan curve in fig. 4) and with the ferritic insert compensated field ripple (blue curve in fig. 4) are practically identical indicating that the ripple is well optimized for scenario 2. With the uncompensated ripple (green curve in fig. 4) a small amount of losses appear from deeper inside the plasma but the amount of extra lost power, about 10% more compared to the optimized case, can be handled well by the plasma facing components. When the TBMs (red curve in fig. 4) are taken into account in scenario 2 the fusion-born alpha particle losses increase by 35% but the loss region is very similar to the one with the compensated ripple.

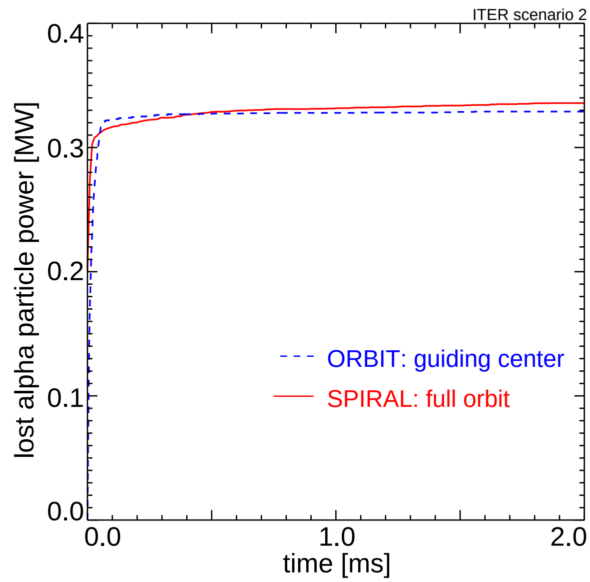

FIG. 5: *Comparison between losses obtained from the guide center following code ORBIT (blue) and the full orbit code SPIRAL (red) for scenario 2 with uncompensated ripple (no ferritic inserts) and no TBMs.*

The losses in scenario 4 appear from deeper inside the plasma than for scenario 2 as can be seen in fig. 4b where losses occur from as deep as $\Psi_{\rm pol} = 0.5$ (or $r/a = 0.68$) for the no ripple case (cyan curve in fig. 4) and the ferritic inserts compensated ripple case (blue curve in fig. 4). When the uncompensated ripple is used (green curve in fig. 4), however, losses occur from much deeper in the plasma, well inside the $\Psi_{\rm pol} = 0.2$ (or $r/a = 0.4$) radius. These losses appear from the well known ripple-loss well for trapped particles at the plasma low field side. When the three TBMs are included with the ferritic inserts compensated ripple field (red curve in fig. 4) the losses increase slightly and there is a sign that losses start to occur from deeper inside the plasma, up to $\Psi_{\rm pol} = 0.3$ (or $r/a = 0.5$) indicating that the compensated ripple field is close to the Goldston-White-Boozer (GWB) loss threshold [14] for scenario 4. In fig. 4b it can also be seen that the alpha particle distribution after 2 ms (dotted curves) is significantly different from the birth profile. This broadening of the alpha particle pressure profile is caused by finite orbit width effects, and not by the transport of alpha particles from the core.

In order to investigate how close the compensated ripple field is to the GWB threshold for scenario 4 we have launched 20000 alpha particles in an annulus between $\Psi_{\rm pol} = 0.35$ to 0.40 and followed those particles for 2 ms at various levels of the ripple field (fig. 6). In this

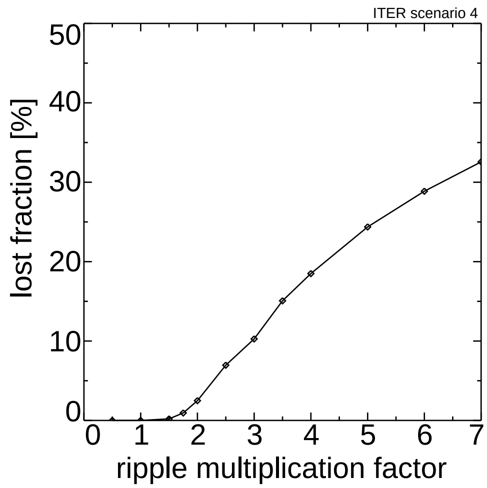

FIG. 6: *Lost fraction of trapped particles after 2 ms from particles launched in an annulus between* $\Psi_{\rm pol} = 0.35$ *and 0.40 for scenario 4 as function of the multiplication factor of the ripple optimized with ferritic inserts. The trapped fraction is 45% of the total alpha particle population at birth in this annulus.*

calculation we have taken the ripple field with ferritic inserts and multiplied it by up to a factor seven. At this location only the trapped particles, which amount to 45% of the total population, are sensitive to the ripple and can potentially be lost from the plasma. In fig. 6 it can be seen that when the ripple field is twice the optimized value, losses start to occur and the losses increase rapidly with increasing ripple. In these calculations the ripple fields due to the TBMs were not included.

For an accurate estimate of heat loads caused by fusion-born alpha particles the particles should be followed long enough so that they reach the LCF. One way to investigate wheather the integration time is sufficient is to plot the accumulated losses as a function of time as shown in fig. 7 and investigate if the losses saturate. From this figure it can be seen that after 2 ms not all the particles are lost. For calculating heat loads it is important to use the total losses and not the losses found in the simulations with a limited particle-following time. The loss rate can well be described by a decaying exponential $(a + b(1 - \exp(-t/\lambda))$ and therefore, we have fit an exponential to the loss curves obtained in the simulations, where we have used the time interval from 0.2 to 2 ms to avoid interference from the prompt losses which occur on time scales of less than 100 μs.

The loss times, λ, that were found for scenario 2 were 0.5 ms for the full ripple, 0.9 ms for the optimized ripple and 1.0 ms for optimized ripple with TBMs. For scenario 4 these

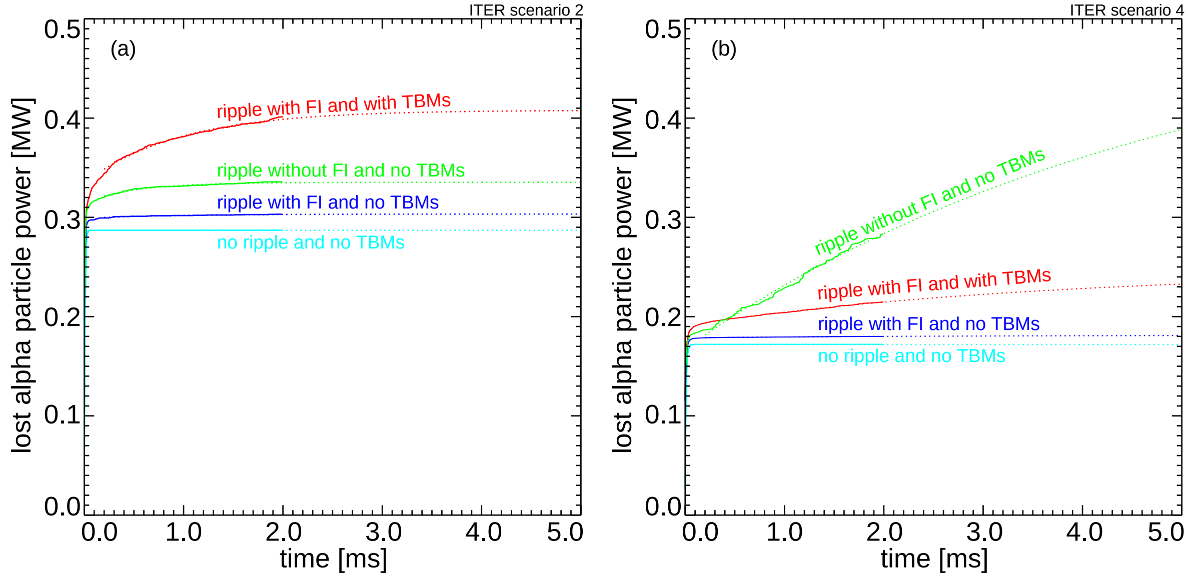

FIG. 7: *Lost alpha particle power as function of time after birth for scenario 2 (a) and scenario 4 (b) for the equilibrium field without ripple and without TBMs (cyan), ripple without ferritic inserts and without TBMs (green), ripple with ferritic inserts and without TBMs (blue) and ripple with ferritic inserts and TBMs. The solid curves are obtained from the SPIRAL code while the dashed curves are exponential extrapolations.*

loss time scales are: 5 ms for the full ripple, 2 ms for the optimized ripple, and 3 ms for the optimized ripple with TBMs. The losses occur on a much faster time scale than the slowing down time which is 1.5 s for scenario 2 and 2.1 s for scenario 4, justifying the choice not to include slowing down effects in the present calculations.

The total lost alpha power due to the ripple fields is 0.5% or less for scenario 2 which has an alpha particle fusion power of 81 MW. For scenario 4 the lost power is 0.3% for the optimized ripple case without TBMs and 0.4% with TBMs while for the unoptimized ripple the losses are about 1%. In scenario 4 the total fusion power is 67 MW. Although the alpha particle losses are small compared to the total fusion power, it is important to investigate where the lost alpha particle power is deposited on the plasma facing components.

We have obtained heat load estimates for the ITER first wall due to fusion-born alpha particles from our simulations. In fact we have calculated the alpha particle heat load on the LCF instead of the wall which is 15 cm away in the vicinity of the plasma mid plane. Because the shape of the first wall is very similar to the LCF (except near the divertor region) we expect that the heat loads at the LCF are a good approximation for the wall

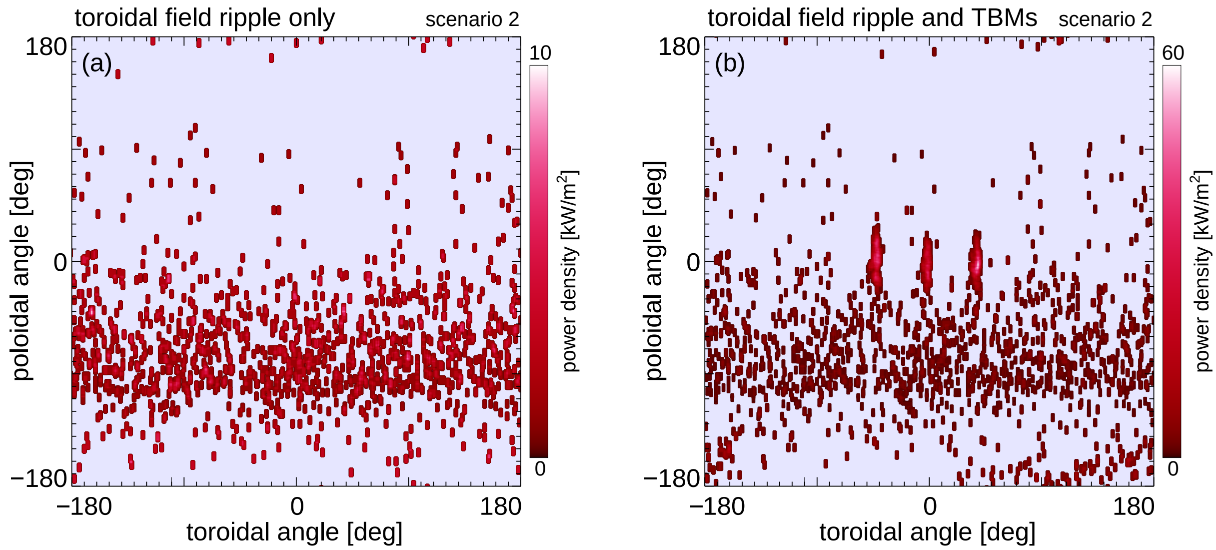

FIG. 8: *calculated heat loads for scenario 2 at the LCF with field ripple only (a) and field ripple and TBMs (b). Note the six fold increase in the power density scale in (b).*

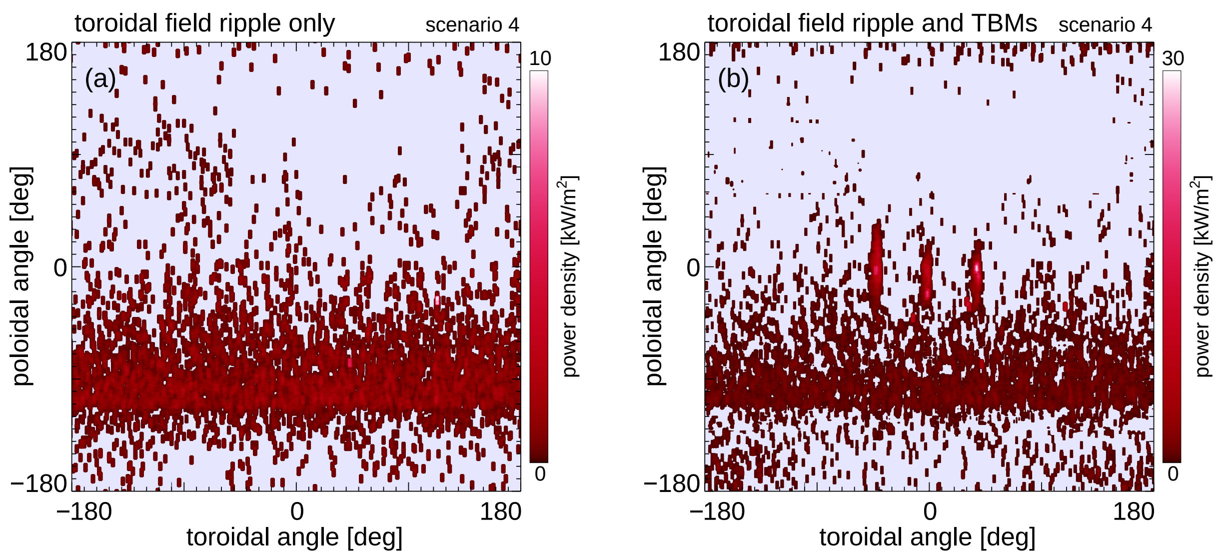

FIG. 9: *calculated heat loads for scenario 4 at the LCF with field ripple only (a) and field ripple and TBMs (b). Note the three fold increase in the power density scale in (b).*

heat loads. In figs. 8 and 9 the heat loads at the LCF are shown as function of toroidal and poloidal angle for scenario 2 and 4. In figs. 8a and 9a the heat loads are shown for the optimized ripple without TBMs and in figs. 8b and 9b with the TBMs included. In the ripple only cases the heat load is spread uniformly near the divertor region with a maximum of 10 kW/m^2 for both scenarios with an estimated uncertainty of 20%. Such heat loads are not threatening to the first wall which is designed to withstand continueous heat loads of up to 500 kW/m^2. When the three TBMs are inserted three localized hot spots appear in front of the TBMs as can seen in figs. 8b and 9b with a maximum heat load of 60 kW/m^2 for scenario 2 and 30 kW/m^2 for scenario 4 and estimated uncertainties of 20%. These hot spots in front of the TBMs are also well below the current design limit for heat loads on the first wall.

The alpha particle heat load is in addition to the heat loads from radiation and neutrons (up to about 200 kW/m^2). In our simulations we have only calculated alpha particle losses due to toroidal field ripple but additional alpha particle losses can be expected from MHD activity (such as Alfvén activity, fishbones, etc.) [15]. An estimate of these increased losses due to MHD is beyond the scope of this paper.

Not only heat loads are an important design limitation for the first wall but also the alpha particle fluency [16]. At high fluencies, typical 10^{22} He/m^2 for proposed materials for the first wall [17], blisters can be formed. At the places with the highest alpha particle heat loads (60 kW/m^2) it will take about 28 hrs to reach the critical fluency for blister formation.

V. CONCLUSION AND OUTLOOK

We have studied fusion born alpha particle losses in ITER that are caused by the (optimized) toroidal field ripple and by the extra field ripple due to three TBMs for two ITER scenarios. For this study we have developed a full particle orbit following code, SPIRAL, which is able to take into account non-axisymmetric ripple fields, such as the ITER ripple field with three TBMs, that cannot be decomposed into a few toroidal harmonics. The SPIRAL code was benchmarked successfully against the well established guide center following code ORBIT and results from both codes agree well for the toroidal field ripple-only cases.

It was found that the toroidal field ripple with the inclusion of ferritic inserts is well optimized for minimizing fusion-born alpha particle losses because the losses that were found in those cases were unavoidable first-orbit losses. It was also found that the optimized ripple field without TBMs is about a factor two below the Goldston-White-Boozer threshold for increased fast ion losses while for scenario 2 this threshold is more than a factor of twenty higher. After adding the three unequally spaced TBMs the alpha particle losses increased by 35% for scenario 2 and 25% for scenario 4.

In addition to total losses the SPIRAL code is also able to estimate heat loads at the last closed flux surface which was used as a good approximation for the first wall. In the optimized toroidal field ripple cases the maximum heat loads of up to 10 kW/m^2 were found in the lower part of the machine near the divertor region for both scenarios. When the ripple fields of the TBMs were added, hot spots emerged in front of the TBMs due to fusion-born alpha particles with maximum heat loads of 60 kW/m^2 and 30 kW/m^2 in scenario 2 and 4 respectively. These heat loads are well below the design value for heat loads on the ITER first wall of 500 kW/m^2. The alpha particle wall loading, however, might restrict the life time of the plasma facing components to days or weeks due to blister formation in front of the TBMs where hot spots are created.

In this study we have only investigated the ripple-induced fusion-born alpha particle losses. It is expected that plasma fluctuations such as MHD activity and turbulence will increase the losses. Therefore, the alpha particle heat loads that we have found in this study are probably lower limits and the loads may increase when plasma fluctuation effects are taken into account.

Acknowledgments

This report was prepared as an account of work by or for the ITER Organization. The Members of the Organization are the People's Republic of China, the European Atomic Energy Community, the Republic of India, Japan, the Republic of Korea, the Russian Federation, and the United States of America. The views and opinions expressed herein do not necessarily reflect those of the Members or any agency thereof. Dissemination of the information in this paper is governed by the applicable terms of the ITER Joint Implementation Agreement. This work is supported by U.S. Department of Energy Contract No.DE-aC02-76-CHO3073.

---

[1] SABIENE, G., personal communication (2007) and CALCOLI, L.T., ROCHELLA, M., Ripple reduction using SS430 Fe inserts, Frascati, (2007)

[2] KONOVALOV, S.V., et al., Energetic Particle Ripple Loss in ITER, Proc. 28th EPS Conf. on Control. Fusion and Plasma Physics, (Funchal-Madeira, Portugal, 2001)

[3] TOBITA, K., et al., Plasma Phys. Control. Fusion **45** (2003) 133

[4] GRIBOV, Y., Plasma of ITER Scenario 2 (2006), and Plasma of ITER Scenario 4 (2006), ftp://pfctrl@ftp.jp.iter.org/array1/PF_control/EQDSK_files/Code PET/

[5] AMOSKOV V., et al., Optimization of distribution of ferromagnetic inserts assuming all sectors of the vacuum vessel to be identical either to the regular sector S-01 or irregular sector S-03, Saint Petersbutg Compagny Energopul LTD, ITER report ITER_D_2FTPWY, (2008)

[6] WHITE, R.B. and CHANCE, M.S., Phys. Fluids **27** (1984) 2455

[7] WHITE, R.B., The Theory of Toroidally Confined Plasmas, Imperial College Press, (2006)

[8] L.L. Lao, J.R. Ferron, R.J. Groebner, W. Howl, H. St. John, E.J. Strait, and T.S. Taylor, Nucl. Fusion **30**, 1035 (1990).

[9] Arfken, G., Mathematical Methods for Physicists, Academic Press, (1970)

[10] FORD, B., and POOL, J.C.T., The evolving NAG Library Service. Sources and Development of Mathematical Software (Ed. Cowell, W.), Prentice-Hall, (1984) http://www.nag.com

[11] HALL, G., and WATT, J.M. (Ed.), Modern Numerical Methods for Ordinary Differential Equations, Oxford University Press, (1976)

[12] T. KURKI-SUONIO, et al., Proc. 22nd IAEA Fusion Energy Conf. (Geneva, Switzerland, 13-18 Oct 2008) (Vienna: IAEA) Paper P6-2 (2008)

[13] K. SHINOHARA, et al., et al., personal communication (2008)

[14] GOLDSTON, R.J., WHITE, R.B., and BOOZER, A.H., Phys. Rev. Lett. **47**, 647 (1981).

[15] FU, G.Y., and DAM J.W., Phys. Fluids **1** (1989) 1949

[16] TOBITA, K., et al., Fusion Eng. Des. **65** (2003) 561

[17] UEDA, Y., et al., J. Nucl. Mater. **313-316** (2003) 32

The Princeton Plasma Physics Laboratory is operated
by Princeton University under contract
with the U.S. Department of Energy.

Information Services
Princeton Plasma Physics Laboratory
P.O. Box 451
Princeton, NJ 08543

Phone: 609-243-2750
Fax: 609-243-2751
e-mail: pppl_info@pppl.gov
Internet Address: http://www.pppl.gov